



ASSESSMENT OF THE FAILURE OF SELF-COMPACTING CONCRETES DIFFERING IN THEIR AIR PORE STRUCTURE BY ACOUSTIC TECHNIQUES

Tomasz GORZELAŃCZYK, Jerzy HOŁA
Institute of Building Engineering, Wrocław University of Technology, Poland

ABSTRACT

The paper presents the results of research on the failure of self-compacting concretes, differing in their air pore structure, subjected to momentary compression. Acoustic techniques, i.e. the acoustic emission technique and the ultrasonic technique, were used to investigate the process. Two self-compacting concretes made from concrete mixes modified with two different superplasticizers (commonly used for this purpose) were tested. The structure of porosity was examined (in the full range of pore diameters) using a computer image analyzer and a mercury porosimeter. The levels of crack initiating stress σ_i and critical stress σ_{cr} , demarcating the particular stages in the failure process and being the visual measure of the latter, were determined. By proving that the levels and the parameters characterizing the air pore structure are interrelated it has been demonstrated that the pore structure has a bearing on the failure of the investigated concretes. Calculation analyses of the fatigue strength of the concretes based on the obtained results are included. The analyses show the results to be useful for building practice.

Keywords: acoustic emission, ultrasonic technique, air pore structure, self-compacting concrete

1. INTRODUCTION

The aim of the research was to assess the failure of self-compacting concretes, differing in their air pore structure, under momentary compression and to determine the levels of crack initiating stress σ_i and critical stress σ_{cr} . One should note that the level of stress σ_i is equated with the fatigue strength of concrete [5]. Acoustic techniques, i.e. the acoustic emission technique and the ultrasonic technique, were used for the purpose. Such research seems necessary considering that self-compacting concrete is increasingly used in construction [1, 2]. Knowing what effect air pore structure has on a given concrete one can determine the latter's proper composition, especially its superplasticizer content which significantly affects the formation of an air pore structure, particularly in building structures subjected to dynamic loads.

2. DESCRIPTION OF THE INVESTIGATIONS

Two self-compacting concretes (designated respectively as A_k and C_k), made from Portland cement CEM I 42.5 R, rounded aggregate with a maximum grading of 16 mm, river sand, silica fumes, two different superplasticizers and drinkable tap water, were investigated. Concrete A_k was made using superplasticizer Addiment FM 34 and concrete C_k using superplasticizer Viscocrete 3. The superplasticizers are commonly used in self-compacting concrete mixes. The compositions of the designed concrete mixes are given in [3]. The specimens made from the mixes were naturally cured for 90 days in a climatic chamber. Average compressive strength $f_{cm,90}$ of the concretes, determined during the investigations, was: 44.52 MPa for concrete A_k and 59.24 MPa for concrete C_k .

50×50×100 mm cuboid specimens cut out from larger test pieces were used for the acoustic emission (AE) investigations. The rate of acoustic events (N_{ev}) and the RMS signal were the AE descriptors recorded during the compression of the specimens. The investigations were carried out on a test stand (fig. 1) which included Vallen-Systeme GmbH AMS3 equipment for measuring acoustic emission and an Instron 1126 testing machine.

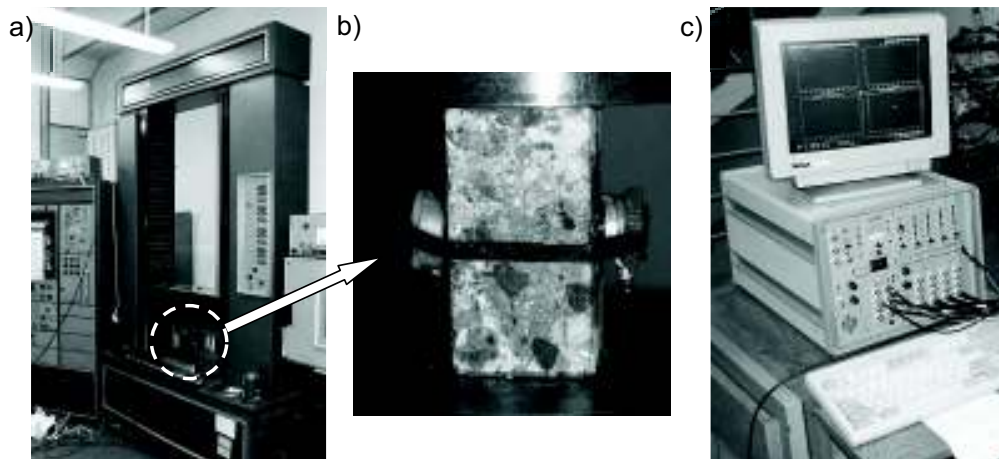


Fig. 1. Stand for measuring acoustic emission in concrete under compression: a) Instron 1126 tester, b) concrete specimen prepared for testing, c) Vallen-Systeme GmbH AMS3 measuring set.

100×100×100 mm concrete specimens were used for the ultrasonic investigations. Longitudinal ultrasonic wave velocity V_L , determined perpendicularly to the direction of load action, versus compressive stress increment was the investigated parameter.

An Image Pro Plus 4.1 analyzer was used to examine and analyze the structure of air pores (in a diameter range of 10 - 4000 μm) in hardened concrete. The setup is shown in fig. 2. The determined structural parameters were: the total air content in

hardened concrete (A), the fraction of micropores less than 0.3 mm in diameter (A_{300}), air pore distribution index \bar{L} and the specific surface of air pores (α).

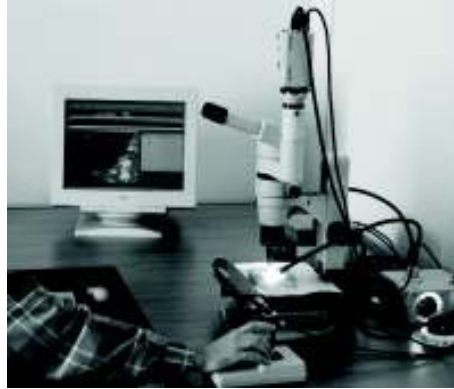


Fig. 2. Setup for investigating air pore structure in hardened concretes.

The air pore characteristic and structure in a pore radius range of 5–7500 nm were investigated using a Carlo Erba Strumentazione model 2000 porosimeter. The following were determined: total porosity p , pore specific volume V , average pore radius \bar{r} , the specific surface of pores (α).

3. EXPERIMENTAL RESULTS AND THEIR ANALYSIS

An exemplary rate of AE events (N_{ev}) registered during the compression of concretes A_k and C_k is shown in fig. 3. The figure also shows relative compressive stress/failure time (σ_c/f_c) graph for the criteria defined in [4]. The levels of crack initiating stress σ_i and critical stress σ_{cr} were determined. According to the literature on the subject, concrete under compression fails in three stages and stresses σ_i and σ_{cr} delimit the particular stages of failure. Stress σ_i marks the boundary between the stable initiation of cracks and the stable propagation of cracks while stress σ_{cr} marks the boundary between the stable propagation of cracks and catastrophic failure [4].

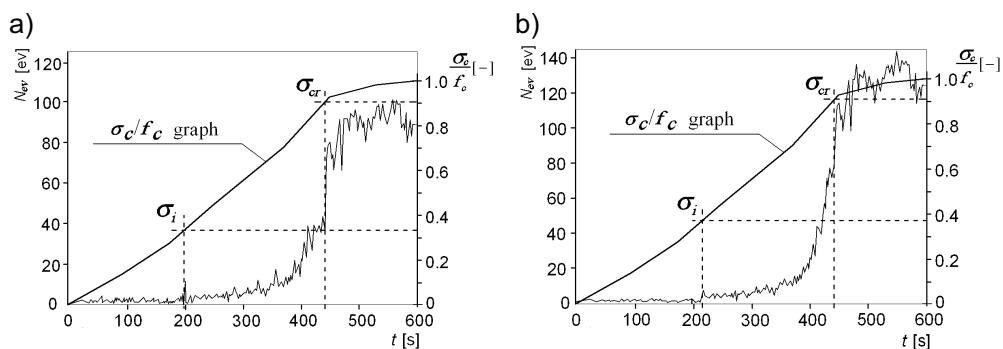


Fig. 3. AE events rate N_{ev} registered during failure of concretes A_k and C_k and relative compressive stress/failure time graph for: a) concrete A_k , b) concrete C_k .

Figure 4 shows longitudinal ultrasonic wave velocity/relative compressive strength increment graphs for self-compacting concretes A_k and C_k as well as the determined levels of stress σ_i and σ_{cr} . According to the criteria given in [4], the stress level at which the longitudinal ultrasonic wave velocity markedly decreases corresponds to the level of crack initiating stress σ_i . The level of stress at which the velocity of longitudinal ultrasonic waves no longer can be measured is equated with the level of critical stress σ_{cr} .

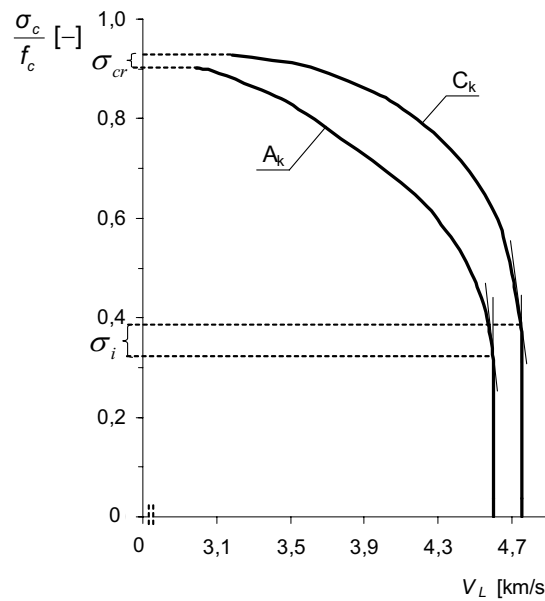


Fig. 4. Longitudinal ultrasonic wave velocity in compressed concretes A_k and C_k versus relative stress increment.

For the investigated concretes the levels of crack initiating stress σ_i and critical stress σ_{cr} , marked in the figs 3 and 4, are shown in table 1. The table also shows (relative and absolute) mean values of stress σ_{im} and σ_{cm} , calculated from the results obtained using the two investigative techniques.

Table 1. Levels of stress σ_i and σ_{cr} and (relative and absolute) values of stress σ_{im} and σ_{cm} in concretes A_k and C_k , determined by ultrasonic technique and acoustic emission technique.

Concrete designation	Measuring technique				Mean values			
	Acoustic emission		Ultrasonic		σ_{im}		σ_{cm}	
	σ_i [-]	σ_{cr} [-]	σ_i [-]	σ_{cr} [-]	[-]	MPa	[-]	MPa
A_k	$\frac{0.33}{4.3\%}$	$\frac{0.91}{3.3\%}$	$\frac{0.33}{8.7\%}$	$\frac{0.90}{2.1\%}$	0.330	15.58	0.905	40.51
C_k	$\frac{0.38}{2.7\%}$	$\frac{0.92}{1.3\%}$	$\frac{0.38}{6.4\%}$	$\frac{0.94}{2.1\%}$	0.380	22.27	0.930	55.29

Note: coefficients of variation are given under the bar.

Table 2 shows the results of air pore structure investigations for concretes A_k and C_k .

Table 2. Results of air pore structure investigations for concretes A_k and C_k .

Investigated parameter	Concrete designation	
	A_k	C_k
Total air content in hardened concrete, A [%]	6.70	2.90
Fraction of micropores with less than 0.3 mm diameter, A_{300} [%]	1.50	0.70
Air pore distribution index \bar{L} [mm]	0.26	0.33
Specific surface of air pores, α [mm ⁻¹]	17	21
Total porosity p [%]	12.71	11.90
Specific volume of pores, V [mm ³ /g]	24.08	17.85
Average radius of pores, \bar{r} [nm]	3.90	6.15
Specific surface of pores, α' [m ² /g]	7.12	2.66

In order to demonstrate the effect of air pores on the failure of the investigated self-compacting concretes, graphs showing the relationships between the average relative levels of crack initiating stress σ_{im} and critical stress σ_{crm} and such structural parameters as: total air content A (fig. 5a), pore distribution index \bar{L} (fig. 5b), total porosity p (fig. 6a), and pore specific surface α' (fig. 6b) are presented in figs 5 and 6.

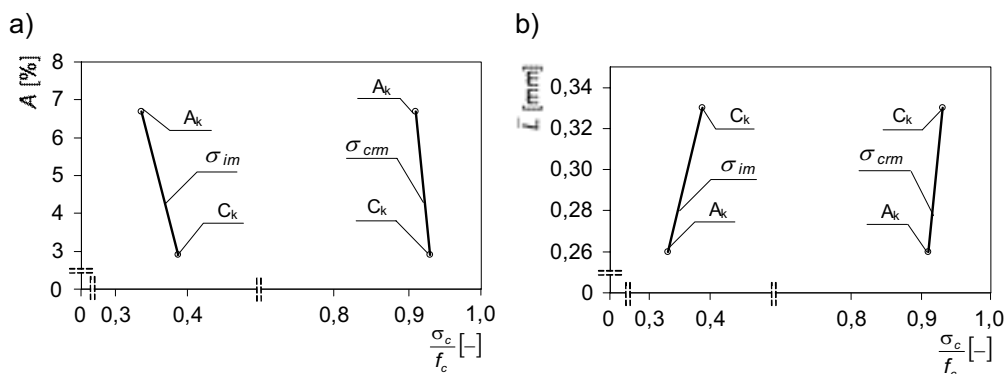


Fig. 5. Relationship between relative levels of stress σ_{im} and σ_{crm} in concretes A_k and C_k and: a) total air content A , b) pore distribution index \bar{L} .

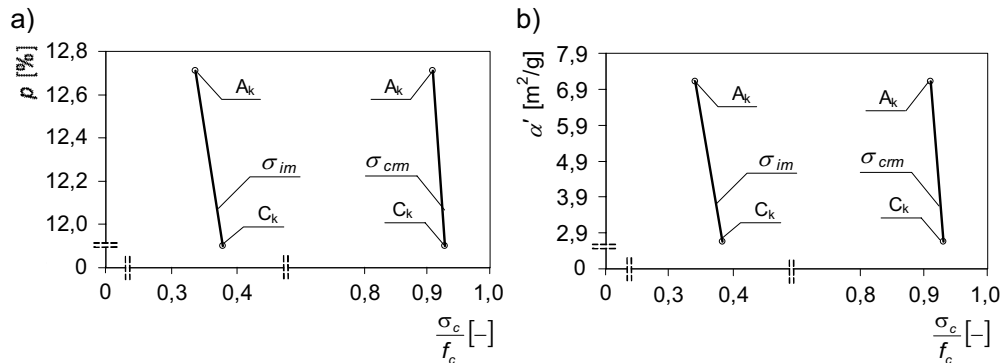


Fig. 6. Relationship between relative levels of stress σ_{im} and σ_{crm} in concretes A_k and C_k and: a) total porosity p , b) pore specific surface α' .

According to figures 5 and 6, the lower the air content in hardened concrete and the larger the interpore distance, and the fewer pores there are in the concrete structure and the smaller their specific surface, the structure is generally more homogeneous.

According to [5], the levels of crack initiating stress σ_i and critical stress σ_{cr} in concrete have a bearing on the life and operational safety of the structures made of the concrete which are subjected to dynamic loads.

On the basis of [5] and experimentally determined levels of crack initiating stress σ_i and critical stress σ_{cr} the following relation for calculating the fatigue strength of self-compacting concrete under compression was adopted:

$$f_c^f / f_c = CN^{-A} (1 + B\rho^f \log N) C_f, \quad (1)$$

where:

C – a ratio of dynamic to static strength at a one-time load (in accordance with [5], it was assumed to be equal to 1.16),

ρ^f – a stress ratio,

σ_c^{\min} – a minimum cycle stress,

σ_c^{\max} – a maximum cycle stress,

C_f – a coefficient expressing the effect of the frequency of load changes on fatigue strength,

A, B – coefficients representing concrete structure condition through their dependence on stress σ_i and σ_{cr} .

Stress ratio ρ^f is expressed as:

$$\rho^f = \sigma_c^{\min} / \sigma_c^{\max}, \quad (2)$$

Coefficient C_f can be expressed as:

$$C_f = 1 + 0.07(1 - \rho^f) \log f, \quad (3)$$

where f is a load change frequency [Hz] and coefficients A and B can be calculated from relations (4) and (5)

$$A = 0.008 - 0.118 \log(\sigma_i / f_c), \quad (4)$$

$$B = 0.118(\sigma_{cr} / \sigma_i - 1). \quad (5)$$

Figure 7 shows the fatigue strength, as a function of the number of stress cycles (N) and stress ratio ρ^f and load change frequency f , calculated using relation (1) for concretes A_k and C_k against that of exemplary ordinary concrete ($f_{cm,90}=42.3$ MPa, $w/c=0.56$, sand content: 37.5%).

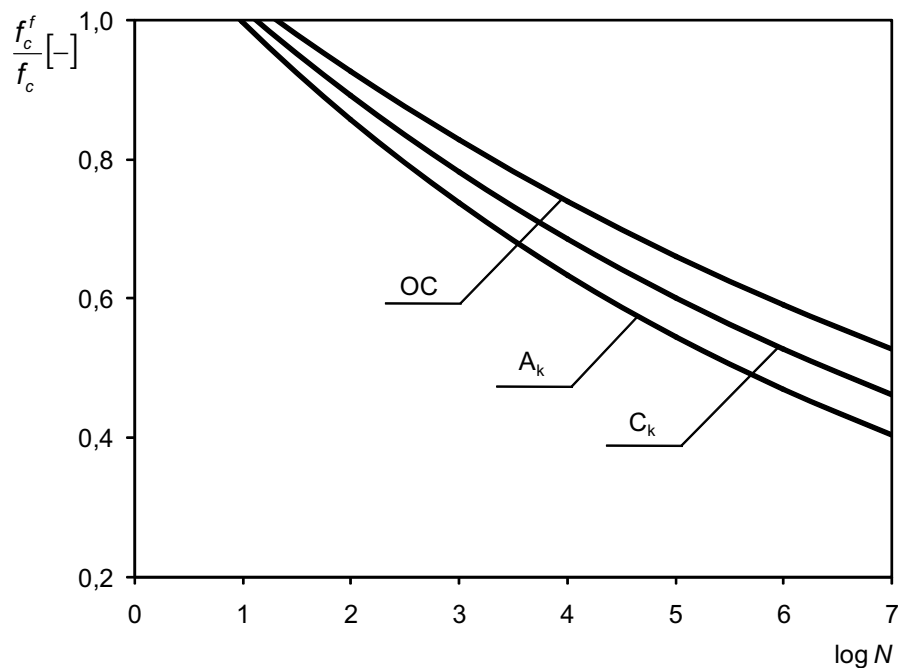


Fig. 7. Calculated fatigue strength of concretes A_k , C_k and OC versus stress cycles at $\rho^f = 0$ and $f = 1$ Hz.

According to the above comparison, the fatigue strength of the self-compacting concretes is lower than that of the ordinary concrete. This is due to their composition, particularly to the high fine aggregate and dust fractions. When self-compacting concretes A_k and C_k are compared, it becomes apparent that their fatigue strength is not

dentically it can be concluded that fatigue strength depends on the air pore structure which in turn depends on the superplasticizer used to modify the concrete. In the case of the investigated self-compacting concretes the series C_k concrete with an admixture of superplasticizer Viscocrete 3 has a higher fatigue strength than that of the series A_k concrete with an admixture of superplasticizer Addiment FM 34.

4. CONCLUSION

The investigations have shown that the air pore structure in the self-compacting concretes affects their failure under a compressive load. It has been demonstrated that lower air content A , lower total porosity p , smaller air pore specific surface α' and higher air pore distribution index \bar{L} are reflected in mainly higher levels of crack initiating stress σ_i and slightly elevated levels of critical stress σ_{cr} . Considering that stress σ_i is equated with the fatigue strength of concrete [5] it is apparent that concrete modified with superplasticizer Viscocrete 3 is more suitable for structural components which are to work under dynamic loads. On the other hand the comparison of the calculated fatigue strengths of the investigated self-compacting concretes and the exemplary ordinary concrete has shown that self-compacting concrete's fatigue strength is lower. This means that structural components made of self-compacting concrete may fail after a smaller number of stress cycles when subjected to dynamic loads.

REFERENCES

- 1 Okamura H, Maekawa K, Mshma T. Performance Based Design for Self Compacting Structural High-Strength Concrete. AC Materials Journal, vol. 28, 2005, 13-34.
- 2 Uts S, Jonasson J, Walin K, Ekman T. Development of SCC for civil engineering applications. Proceeding PRO33 - 3rd International RILEM Symposium Self Compacting Concrete. RILEM Publications S.A.R.L. 2003, 567-575.
- 3 Gorzelańczyk T, Hoła J. Assessment of the Destruction Process of Prestressed Self-Compacting Concrete by Acoustic Methods [in Polish]. Proceeding of the 34th KKBN Domestic Conference on Nondestructive Tests, Zakopane, 2005, 234-237.
- 4 Hoła J. Determination of Initiating and Critical Stress Levels in Compressed Plain and High-strength Concrete by Acoustic Methods. Archives of Acoustics, Vol. 25, 2000, pp.57-65.
- 5 Furtak K. Load Capacity of Normal Cross-section of Bent Reinforced Concrete Elements Subjected to Changing Loads, as Applied Particularly to Bridges [in Polish]. Scientific Papers of Cracow Polytechnic, No. 4, 1985.

This research was carried out as part of KBN project no. 4 T07E 020 28 entitled "Research into Deformability and Failure of Self-compacting Concretes".